

Theory of Half-Metallic Ferrimagnetism in Double Perovskites

Onur Erten,¹ O. Nganba Meetei,¹ Anamitra Mukherjee,¹ Mohit Randeria,¹ Nandini Trivedi,¹ and Patrick Woodward²

¹*Department of Physics, The Ohio State University, Columbus, Ohio 43210, USA*

²*Department of Chemistry, The Ohio State University, Columbus, Ohio 43210, USA*

(Received 6 July 2011; published 13 December 2011)

Double perovskites such as $\text{Sr}_2\text{FeMoO}_6$ are rare examples of materials with half-metallic ground states and a ferrimagnetic T_c above room temperature. We present a comprehensive theory of the temperature and disorder dependence of their magnetic properties by deriving and validating a new effective spin Hamiltonian for these materials, amenable to large-scale three-dimensional simulations. We show how disorder, ubiquitous in these materials, affects T_c , the magnetization, and the conduction electron polarization. We conclude with a novel proposal to enhance T_c without sacrificing polarization.

DOI: [10.1103/PhysRevLett.107.257201](https://doi.org/10.1103/PhysRevLett.107.257201)

PACS numbers: 75.47.Lx, 72.80.Ga, 75.10.-b, 75.50.Gg

There are very few examples of materials that exhibit half-metallic ground states, with fully spin-polarized conduction electrons, together with a ferromagnetic T_c above room temperature. This combination of properties has the potential for an enormous technological impact in spintronic applications such as tunneling magnetoresistance devices. The two classes of materials that offer the most promise for room-temperature applications are double perovskites and Heusler alloys, both of which have several examples with T_c well above room temperature.

The double perovskites (DPs) are of particular interest since the perovskite family shows an amazingly rich variety of properties, including colossal magnetoresistance, multiferroic behavior, and high T_c superconductivity. In the long run, the ability to make heterostructures of such multifunctional oxides is likely to open up very interesting possibilities, provided the stoichiometry and ordering of these materials can be controlled.

One of the best-studied half-metallic DPs is $\text{Sr}_2\text{FeMoO}_6$ (SFMO) with $T_c \approx 420$ K, well above room temperature [1–3]. SFMO is but one example of a DP $A_2BB'O_6$, which is derived from the simple ABO_3 perovskite structure by a three-dimensional (3D) checkerboard ordering of B and B' ions.

From a theoretical point of view, we argue that DPs are simple systems for understanding metallic ferromagnetism, despite their apparent complexity. First, in contrast to ferromagnets like iron, there is a clear separation of the localized (B) and itinerant degrees of freedom (coming from B') in the DPs. Second, in contrast to the manganites, DPs have neither Jahn-Teller distortions nor, given the large separation between B sites, antiferromagnetic superexchange that competes with double exchange. This, in fact, is the main reason for the higher T_c 's in the DPs compared with the manganites. Third, in contrast to dilute magnetic semiconductors, disorder is not an essential aspect of the theoretical problem.

Previous theoretical work on half-metallic DPs includes pioneering $T = 0$ electronic structure calculations [2,3]

and model Hamiltonians analyzed using various mean-field theories [4–6] and two-dimensional (2D) simulations [7]. In this Letter, we present a comprehensive theory that gives insight into the temperature and disorder dependence of the magnetic properties of half-metallic DPs. We make detailed comparisons with and predictions for SFMO.

Our main results are the following. (1) We show that both the total magnetization $M(T)$ and the conduction electron polarization $P(T)$ at E_f are proportional to the magnetization $M_S(T)$ of localized Fe spins. This result is significant because, while $M(T)$ is much simpler to measure than $P(T)$, the latter is of crucial importance for spintronic applications. (2) Our main theoretical advance is the derivation and validation of an effective classical spin Hamiltonian H_{eff} [see Eq. (2)] for DPs, which differs from both the Heisenberg and Anderson-Hasegawa models [8]. We show that H_{eff} describes the full T dependence of the magnetization $M_S(T)$ and in turn that of $M(T)$ and $P(T)$. (3) We present the results of simulations of H_{eff} on large 3D lattices, including disorder effects, thus going beyond all previous theoretical calculations on SFMO. (4) We compute $M(T)$ and T_c , using microscopic band-structure parameters as input, and see how these are affected by deviations from stoichiometry and by antisite (AS) disorder, ubiquitous in real materials. Ours is the first theory to show that T_c is insensitive to AS disorder, in excellent agreement with experiments, even though $M(0)$ is suppressed. (5) We conclude with a novel proposal to increase T_c of SFMO, which in turn enhances the polarization $P(T)$ at high temperatures, by using a combination of excess-Fe disorder and La doping to maintain carrier density.

Model Hamiltonian.—For a large Hund's coupling J_H , the Fe^{3+} ($3d^5$) site has an $S = 5/2$ “core spin” or local moment. The Mo^{5+} ($4d^1$) contributes a t_{2g} electron, which hybridizes via O with the Fe t_{2g} states. Symmetry implies that $d_{\alpha\beta}$ electrons delocalize only in the (α, β) plane [9]. Thus, the motion of electrons in the 3D system decouples into three 2D planes. The “double-exchange” Hamiltonian

[5,7] describing itinerant electrons interacting with core spins is

$$H = -t \sum_{\langle i,j \rangle, \sigma} (\epsilon_{i\sigma} d_{i\sigma}^\dagger c_{j\sigma} + \text{H.c.}) - t' \sum_{\langle i,j' \rangle, \sigma} c_{j'\sigma}^\dagger c_{j\sigma} + \Delta \sum_i d_{i\downarrow}^\dagger d_{i\uparrow}. \quad (1)$$

Here, $d_{i\sigma}$ ($c_{i\sigma}$) are fermion operators on the Fe (Mo) sites with spin σ . At the Fe sites i , we choose local axes of quantization along \mathbf{S}_i and Pauli exclusion prohibits an \uparrow electron. For all the Mo sites j , we choose the same (global) axis of quantization. The orientation (θ_i, φ_i) of the classical spins \mathbf{S}_i then affects the Mo-Fe hopping via $\epsilon_{i\uparrow} = -\sin(\theta_i/2) \exp(i\varphi_i/2)$ and $\epsilon_{i\downarrow} = \cos(\theta_i/2) \times \exp(-i\varphi_i/2)$.

The parameters in H are the hopping amplitudes t between nearest-neighbor (Fe-Mo) sites, t' between two Mo sites, and the charge transfer energy Δ between Fe $t_{2g\downarrow}$ and Mo t_{2g} states; see Fig. 1(a). For now, we choose $t = 1$ as our unit of energy [10]. Symmetry dictates $t' > 0$. We choose $t'/t = 0.1$ and $\Delta/t = 2.5$, using realistic band parameters for SFMO as input [3]. We will show below that t sets the scale for the magnetic T_c and that choosing $t = 0.27$ eV, consistent with Ref. [3], leads to the experimental $T_c = 420$ K of SFMO.

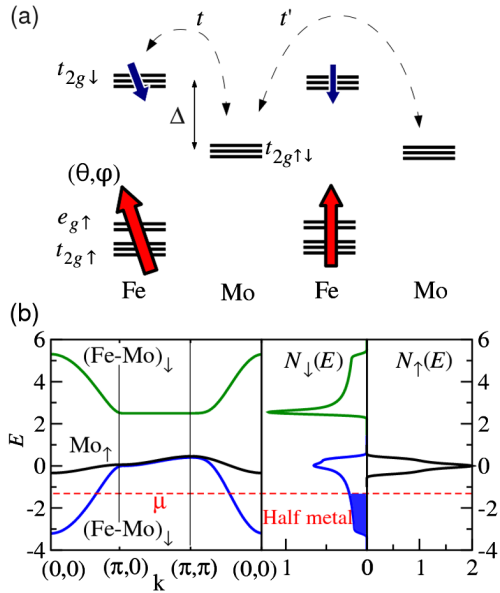


FIG. 1 (color online). (a) Schematic showing energy levels at transition metal sites in two unit cells (formula units) of SFMO. The Fe sites have localized $S = 5/2$ core spins, treated as classical vectors with orientation (θ, φ) . The parameters t , t' , and Δ of the Hamiltonian (1), governing the dynamics of the itinerant electrons in t_{2g} orbitals, are also shown. (b) Calculated electronic structure $E(\mathbf{k})$ and the spin-resolved DOSs $N_\downarrow(E)$ and $N_\uparrow(E)$ in the ferrimagnetic ground state with all core spins up. Note the half-metallic ground state in SFMO with conduction electrons polarized opposite to core spins.

We use exact diagonalization (ED) to solve the quantum mechanics of “fast” itinerant electrons moving in the background of “slow” $S = 5/2$ spins, for which we use a $T \neq 0$ classical Monte Carlo (MC) simulation. The separation of time scales is justified below. Using standard ED-MC techniques, supplemented by $T = 0$ variational calculations, we obtain the results shown in Figs. 1 and 2. These results are limited to 2D systems because of the computational cost of ED. We will present below results on large 3D systems using a different technique.

We show in Fig. 1(b) the band structure and the spin-resolved density of states (DOS) $N_\sigma(E)$ for the ferrimagnetic ground state of SFMO with $n = 0.33$ electrons per unit cell per plane. These results are consistent with photoemission experiments [11]. We find that the conduction electrons, with magnetization $M_{\text{el}}(T = 0) = 1 \mu_B$ (per unit cell), are polarized opposite to the Fe spins, with core spin magnetization $M_S(0) = 5 \mu_B$. The half-metallic ground state, with $N_\downarrow(0) = 0$ and $N_\uparrow(0) \neq 0$, has a net magnetization $M(0) = M_S(0) - M_{\text{el}}(0) = 4 \mu_B$.

We see from Fig. 2(a) that $M_S(T)$, $M_{\text{el}}(T)$, and hence the total magnetization $M(T) = M_S(T) - M_{\text{el}}(T)$ all have essentially the same T dependence. Another quantity of great interest is the conduction electron polarization $P(T)$

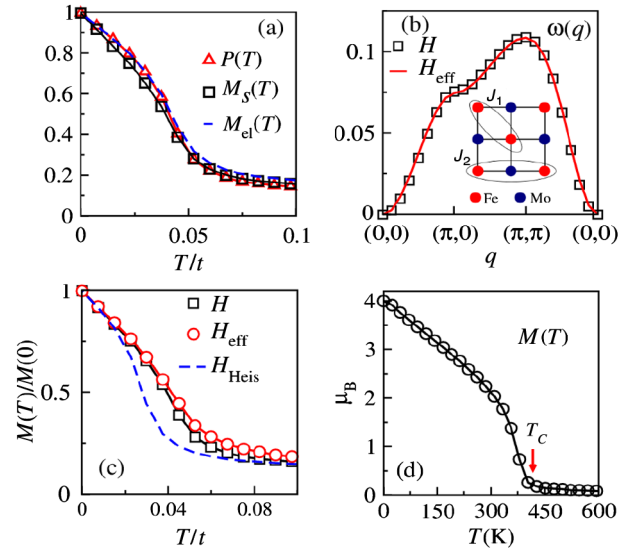


FIG. 2 (color online). (a) The core spin magnetization $M_S(T)$, conduction electron magnetization $M_{\text{el}}(T)$, and polarization $P(T)$ at E_f calculated using the ED-MC method. Both $M_S(T)$ and $M_{\text{el}}(T)$ are normalized to their $T = 0$ values. We conclude that all magnetic properties are proportional to $M_S(T)$. (b) Spin-wave dispersion of the full Hamiltonian H , obtained by exact diagonalization, compared with that of the effective Hamiltonian H_{eff} . Inset: Fe-Mo lattice showing the nearest-neighbor (J_1) and next-nearest-neighbor (J_2) interactions of H_{eff} . (c) The normalized magnetization $M(T)$ for three Hamiltonians: H , H_{eff} , and the Heisenberg model. These results are obtained on 8^2 systems with error bars no larger than the symbol size. (d) Magnetization $M(T)$ from 3D simulations of H_{eff} on 16^3 systems. The infinite system T_c is obtained from finite size scaling [13].

at E_f which determines the tunneling magnetoresistance. This is defined by $P(T) = [N_{\uparrow}(0) - N_{\downarrow}(0)]/[N_{\uparrow}(0) + N_{\downarrow}(0)]$, with $E = 0$ in the DOS measured from E_f . In Fig. 2(a), we also see that $P(T)$ also follows the T -dependent $M_S(T)$.

Effective Spin Hamiltonian.—The results of Fig. 2(a) imply that, if we had a reliable theory for the core spin magnetization $M_S(T)$, we could understand all the magnetic properties of SFMO, including the polarization $P(T)$. With this motivation, we derive an effective Hamiltonian H_{eff} for the core spins by generalizing the two-site Anderson-Hasegawa [8] analysis for manganites to double perovskites.

To derive H_{eff} , we find the exact solution of the full H of Eq. (1) for one electron in two unit cells [12]. For a given t_{2g} symmetry, the Hilbert space has three states per unit cell: Fe $t_{2g\downarrow}$ and Mo $t_{2g,1,\downarrow}$, leading to a 6×6 matrix for two unit cells. We analytically find its lowest eigenvalue as a function of the angle $(\theta_i - \theta_j)$ between core spins. Working in two different geometries, we find [13] the nearest-neighbor (J_1) and next-nearest-neighbor (J_2) interaction energies; see the inset in Fig. 2(b). Expressing these in terms of $\mathbf{S}_i \cdot \mathbf{S}_j$, where each \mathbf{S}_i is a unit vector, we obtain the effective Hamiltonian

$$H_{\text{eff}} = -J_1 \sum_{\langle i,j \rangle} F_1(\mathbf{S}_i \cdot \mathbf{S}_j) - J_2 \sum_{\langle\langle i,j \rangle\rangle} F_2(\mathbf{S}_i \cdot \mathbf{S}_j), \quad (2)$$

where the functions $F_1(x) = 8\sqrt{2 + \sqrt{2 + 2x}}$ and $F_2(x) = (5 + \sqrt{5})\sqrt{6 + 2\sqrt{3 + 2x}}$. Our two-unit cell analysis gives explicit expressions [13] for J_1 and J_2 , both of which are ferromagnetic, with their scale set by the kinetic energy t of delocalization. We emphasize that the double square-root form of H_{eff} is quite different from the (single square-root) Anderson-Hasegawa model.

Next, we need to understand how we can use H_{eff} going beyond the simple two-unit cell derivation. Specifically: (i) How can we relate J_1 and J_2 to t , t' , Δ , and the filling n ? (ii) To what extent does H_{eff} capture the essential physics of the full Hamiltonian H ?

The dependence of J_1 and J_2 on microscopic parameters can be obtained by matching the spin-wave spectra of H_{eff} and H . This comparison is shown in Fig. 2(b) along certain symmetry directions. We find spin-wave dispersion for H using ED to compute the energy of electrons moving in a “frozen” spin-wave background. The low energy scale of $0.1t$ for spin dynamics [see Fig. 2(b)] justifies *a posteriori* our assumption of slow spins and fast electrons, whose bandwidth is of the order of t [see Fig. 1(b)]. The same separation of energy scales also justifies the use of T -independent exchange couplings J_1 and J_2 for all $T < T_c$, as we discuss next.

To validate the effective model H_{eff} , we show in Fig. 2(c) that it reproduces the magnetization $M(T)$ of the full Hamiltonian H over the entire range of temperatures. In contrast, the Heisenberg model H_{Heis} gives quite

different results, except in the $T \rightarrow 0$ limit with small spin deviations. Thus, $M(T)$ for the DP’s cannot be described by a Heisenberg model, while H_{eff} provides an excellent description of the ED-MC result.

The classical H_{eff} can be easily simulated on large 3D lattices, unlike the full H , and the results are shown in Fig. 2(d). We note the linear drop in $M(T)$ at low T , due to classical spin waves, followed by a rapid suppression of M at the phase transition [14]. Our $M(T)$ results are in qualitative agreement with recent experiments [15]. We estimate T_c in the infinite volume limit using the finite size scaling of results obtained on L^3 systems with $L = 8, 12$, and 16 [13]. For $t'/t = 0.1$ and $\Delta/t = 2.5$, we find $T_c = 0.14t$. Comparing this to $T_c = 420$ K for pure SFMO, we obtain $t = 0.27$ eV, consistent with Ref. [3].

Disorder.— H_{eff} permits us to model various kinds of disorder and deviations from stoichiometry [13]. (i) Excess Fe is modeled with an extra spin (at a Mo site) that interacts with its neighboring spins with a large antiferromagnetic (AF) superexchange $S(S+1)J_{\text{AF}} \approx 34$ meV [16]. (ii) Excess Mo is modeled by removing an Fe spin from the lattice. Both (i) and (ii) also require reevaluation of J_1 and J_2 due to the change in carrier density n . (iii) Here, we focus on antisite (AS) disorder, the most common form of disorder in DPs, with Fe and Mo interchanged and no change in n .

We see from Fig. 3 that AS disorder systematically reduces $M(0)$ without affecting T_c , in excellent agreement with experiments [17]. We quantify AS disorder using δ as the fraction of Fe atoms that are on the Mo sublattice. The observed magnetization $M(0)[1 - 2\delta]$ arises from the loss of two moments for each AS defect—one from the moment lost at the Mo (on the Fe sublattice) and the other from the Fe (on the Mo sublattice) antiferromagnetically coupled to its neighbors via J_{AF} .

There are two opposite effects of AS disorder on T_c that appear to balance each other. The strong Fe-Fe superexchange J_{AF} pins the spins surrounding the Fe defect and makes the magnetic order more robust against thermal

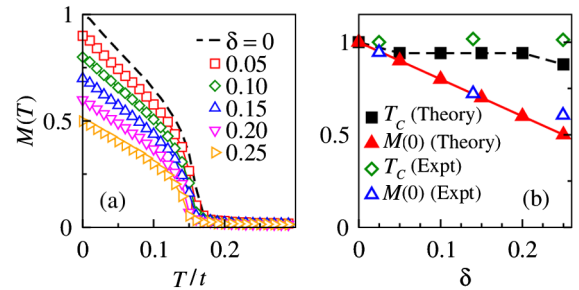


FIG. 3 (color online). (a) $M(T)$, normalized by the $M(0)$ for the disorder-free system, for various values of AS disorder δ (see the text). (b) Theoretical results for T_c and $T = 0$ magnetization $M(0)$ (both normalized with respect to their disorder-free values) compared with experiments [17]. $M(0)$ drops like 2δ , while T_c is insensitive to AS disorder.

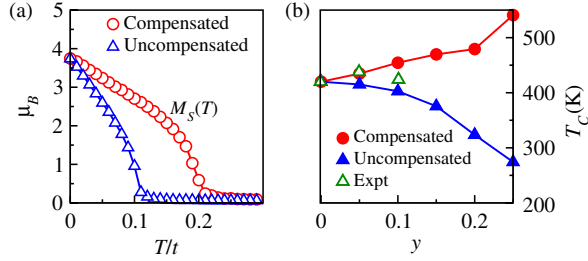


FIG. 4 (color online). (a) Core spin magnetization $M_S(T)$ for $\text{La}_x\text{Sr}_{2-x}\text{Fe}_{1+y}\text{Mo}_{1-y}\text{O}_6$ for uncompensated $(x, y) = (0, 0.25)$ and compensated $(x, y) = (0.75, 0.25)$ Fe-rich systems. (b) The uncompensated $T_c(y)$ is compared with experiments [21]. Our prediction for the compensated ($x = 3y$) system shows large enhancement in T_c .

fluctuations. On the other hand, the Mo defect leads to broken J_1 and J_2 bonds which weaken the magnetism. The net effect is a T_c insensitive to δ for moderate levels of AS disorder, which is exactly what experiments observe. We note that, while the loss of $M(0)$ with AS disorder has been explained earlier [18–20], ours is the first theory to correctly account for $T_c(\delta)$; previous theories either found a drop [18] in T_c or an increase [5].

Raising T_c .—We conclude with a proposal to raise the ferrimagnetic T_c without sacrificing the conduction electron polarization P ; see Fig. 4. In short, it involves adding excess Fe and compensating for the loss of mobile carriers by La substitution on the Sr site.

To see how this works, let us first consider excess Fe without any compensation: $\text{Sr}_2\text{Fe}_{1+y}\text{Mo}_{1-y}\text{O}_6$. In this case, $M_S(0)$ decreases like y due to the AF alignment of excess spins. T_c also decreases with y because the loss of carriers $n = (1 - 3y)/3$ dominates over the enhanced pinning of moments by J_{AF} in the vicinity of defects. For the uncompensated case, the calculated $T_c(y)$ in Fig. 4(b) is in reasonable agreement with experiments [21].

We can compensate for the carriers by A -site substitution: $\text{La}_x\text{Sr}_{2-x}\text{Fe}_{1+y}\text{Mo}_{1-y}\text{O}_6$, with electron density $n = (1 + x - 3y)/3$ per plane. Choosing $x = 3y$ counters the doping-dependent drop in T_c that dominated above, and we find that T_c can be significantly enhanced over that of pure SFMO due to just the local pinning of moments at excess-Fe sites. This increase in T_c goes hand-in-hand with an unchanged $M_S(0)$; see Fig. 4(a).

We also note that the polarization $P(0)$ remains 100%. When the Fe spins cant at finite T , electrons depolarize by the mixing of up and down states; however, no such processes are permitted at $T = 0$, even in a disordered Fe-rich system. We have checked, using the full Hamiltonian (1), that, even though the strict proportionality between $M_S(T)$ and $P(T)$ is not observed in the presence of disorder, the high temperature P is still enhanced over the clean system due to the large increase in T_c .

An alternative way to enhance T_c is to add mobile electrons using La doping, which, however, has been shown to lead to a considerable increase in AS disorder [22]. In principle, compensated doping as proposed here should introduce less AS disorder [13].

In conclusion, while we have focused here on SFMO, our theory provides a general framework for understanding half-metallic ferrimagnetism in DPs. Interesting directions for future work include A -site substitution; Coulomb correlations on B' , which may become increasingly important for larger carrier concentrations; and spin-orbit coupling on B' for $5d$ elements.

We acknowledge support from the Center for Emergent Materials, an NSF MRSEC Grant No. DMR-0820414. We thank D. D. Sarma, R. Mishra, O. Restrepo, and W. Windl for discussions and the Ohio Supercomputer Center for the use of computational facilities.

-
- [1] For a recent review, see D. Serrate, J.M. De Teresa, and M.R. Ibarra, *J. Phys. Condens. Matter* **19**, 023201 (2007).
 - [2] K.I. Kobayashi *et al.*, *Nature (London)* **395**, 677 (1998).
 - [3] D.D. Sarma *et al.*, *Phys. Rev. Lett.* **85**, 2549 (2000).
 - [4] A. Chattopadhyay and A.J. Millis, *Phys. Rev. B* **64**, 024424 (2001).
 - [5] J.L. Alonso *et al.*, *Phys. Rev. B* **67**, 214423 (2003).
 - [6] L. Brey *et al.*, *Phys. Rev. B* **74**, 094429 (2006).
 - [7] P. Sanyal and P. Majumdar, *Phys. Rev. B* **80**, 054411 (2009).
 - [8] P.W. Anderson and H. Hasegawa, *Phys. Rev.* **100**, 675 (1955).
 - [9] A.B. Harris *et al.*, *Phys. Rev. B* **69**, 035107 (2004).
 - [10] Flipping the sign of t only interchanges the bonding and antibonding bands shown in Fig. 1(b).
 - [11] T. Saitoh *et al.*, *Phys. Rev. B* **66**, 035112 (2002).
 - [12] One electron in two unit cells corresponds to $n = 0.5$, the closest we can get to SFMO filling $n = 0.33$ in this geometry. We also ignore t' .
 - [13] Details will be published elsewhere.
 - [14] Note (i) the qualitative difference between the sharp transition found in 3D [Fig. 2(d)] with the smooth behavior in 2D [Fig. 2(c)] and (ii) the factor of 3 difference in T scales between 3D (face-centered cubic) and 2D (square lattice) arising from the increased number of neighbors.
 - [15] A.J. Hauser *et al.*, *Phys. Rev. B* **83**, 014407 (2011).
 - [16] We use $S(S+1)J_{\text{SE}} = k_B T_N/2$ for the AF insulator LaFeO_3 with $T_N = 750$ K.
 - [17] J. Navarro *et al.*, *Phys. Rev. B* **67**, 174416 (2003).
 - [18] A. Ogale *et al.*, *Appl. Phys. Lett.* **75**, 537 (1999).
 - [19] B. Aguilar, O. Navarro, and M. Avignon, *Europhys. Lett.* **88**, 67003 (2009).
 - [20] R. Mishra *et al.*, *Chem. Mater.* **22**, 6092 (2010).
 - [21] D. Topwal *et al.*, *Phys. Rev. B* **73**, 094419 (2006).
 - [22] J. Navarro *et al.*, *Phys. Rev. B* **64**, 092411 (2001).